Chemical Targeting of GAPDH Moonlighting Function in Cancer Cells Reveals Its Role in Tubulin Regulation

Da-Woon Jung,[1,6] Woong-Hee Kim,[1,6] Shinae Seo,[1] Eunsang Oh,[1] Soon-Ho Yim,[2] Hyung-Ho Ha,[3] Young-Tae Chang,[4,5] and Darren Reece Williams[1,*]

[1]New Drug Targets Laboratory, School of Life Sciences, Gwangju Institute of Science and Technology, 1 Oryong-Dong, Buk-Gu, Gwangju 500-712, Republic of Korea
[2]College of Public Health and Welfare, Dongshin University, 185 Geonjaero, Naju, Jeonnam 520-714, Republic of Korea
[3]College of Pharmacy, Sunchon National University, Sunchon 570-742, Republic of Korea
[4]Department of Chemistry and MedChem Program of Life Sciences Institute, National University of Singapore, 3 Science Drive 3, Singapore 117543, Singapore
[5]Laboratory of Bioimaging Probe Development, Singapore Bioimaging Consortium, Agency for Science, Technology and Research (A*STAR), Singapore 138667, Singapore
[6]Co-first author
*Correspondence: darren@gist.ac.kr
http://dx.doi.org/10.1016/j.chembiol.2014.08.017

SUMMARY

Glycolytic enzymes are attractive anticancer targets. They also carry out numerous, nonglycolytic "moonlighting" functions in cells. In this study, we investigated the anticancer activity of the triazine small molecule, GAPDS, that targets the glycolytic enzyme glyceraldehyde 3-phosphate dehydrogenase (GAPDH). GAPDS showed greater toxicity against cancer cells compared to a known GAPDH enzyme inhibitor. GAPDS also selectively inhibited cell migration and invasion. Our analysis showed that GAPDS treatment reduced GAPDH levels in the cytoplasm, which would modulate the secondary, moonlighting functions of this enzyme. We then used GAPDS as a probe to demonstrate that a moonlighting function of GAPDH is tubulin regulation, which may explain its anti-invasive properties. We also observed that GAPDS has potent anticancer activity in vivo. Our study indicates that strategies to target the secondary functions of anticancer candidates may yield potent therapeutics and useful chemical probes.

INTRODUCTION

Glycolysis is the breakdown of glucose into pyruvate to generate ATP. It is an ancient, highly conserved metabolic pathway that developed under anaerobic conditions, i.e., before the appearance of significant levels of photosynthesis-derived oxygen in the atmosphere (Kim and Dang, 2005). Increased glycolysis is a hallmark of cancer cells and is known as the Warburg effect (Warburg et al., 1927). For example, the rate of glycolysis in homogenized tumor tissues is approximately ten times that of normal tissues, which has led to the description of cancer cells as "glycolysis addicts" (Bagley, 2010). The Warburg effect is thought to be a metabolic adaptation to hypoxia that arises during tumorigenesis (Kim and Dang, 2005). This offers a therapeutic strategy to selectively kill cancer cells using glycolysis inhibitors, which can overcome drug resistance to induce cell death (Xu et al., 2005).

The individual enzymes constituting the glycolysis pathway were thought of as "ancient" or "boring" proteins with well-characterized catalytic functions and structural properties (Kim and Dang, 2005). However, over the past decade, this view has been revised, and many glycolytic enzymes are now classified as "moonlighting" proteins (Jeffery, 2009). These proteins carry out additional functions that are unrelated to their originally characterized biological activity. Many examples of moonlighting by glycolytic enzymes have been discovered. Some are related to carcinogenesis. For example, glyceraldehyde 3-phosphate dehydrogenase (GAPDH) can translocate to the cell nucleus, where it has a role in the regulation of apoptosis. This has been linked to the promotion of tumorigenesis (Colell et al., 2009). One mechanism by which nuclear localized GAPDH regulates cell death is via complex formation with promyelocytic leukemia protein (Tristan et al., 2011). Moreover, GAPDH can act as a prosurvival factor by stimulating autophagy-mediated clearance of permeabilized mitochondria (Tristan et al., 2011). Examples of moonlighting by other glycolytic enzymes include lactate dehydrogenase, which was identified as a regulator of gene transcription via association with the Oct-1 coactivator in S-phase (OCA-S) transcription complex (Dai et al., 2008), and enolase, which can be alternatively spliced to regulate transcription of the oncogene, Myc (Subramanian and Miller, 2000).

The triazine-based small molecule, GAPDH segregator (GAPDS), targets GAPDH and was first described in 2007 (Min et al., 2007). GAPDS treatment produced antidiabetic effects in the roundworm, *Caenorhabditis elegans*, and mammalian adipocytes, which demonstrated that GAPDH is a candidate for diabetes drug discovery. In cells, GAPDH forms a tetramer for full enzyme activity. GAPDS binding dissociates the GAPDH tetramer into monomers (Min et al., 2007). GAPDH is upregulated in different cancers and has been linked to numerous
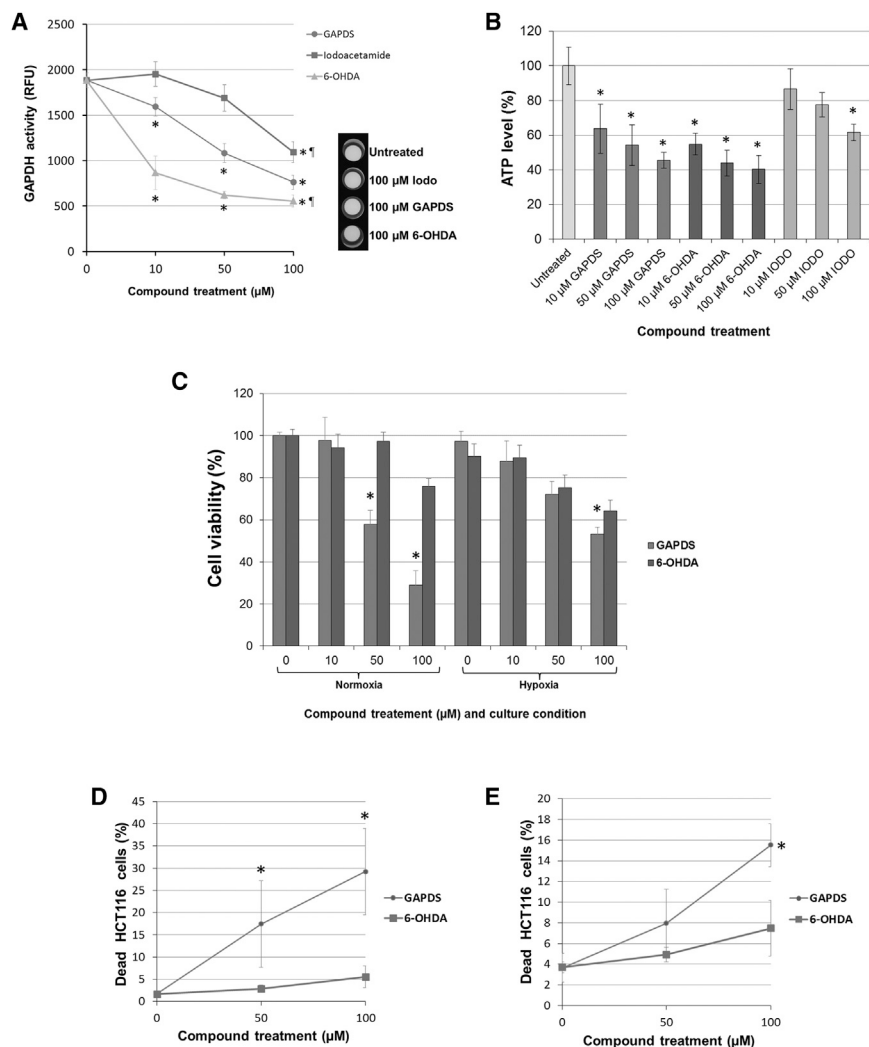
Figure 1. GAPDS Inhibits GAPDH Activity and Reduces Cancer Cell Viability

(A) Effects of GAPDS, 6-OHDA, and iodoacetamide on GAPDH activity in human HCT116 colon carcinoma cells. Cells were incubated with inhibitors for 24 hr. Error bars indicate SD; *p < 0.05 compared to untreated cancer cells. A photograph of the assay plate is included.

(B) Effect of GAPDS, 6-OHDA, and iodoacetamide on ATP levels in human HCT116 colon carcinoma cells. Cells were incubated with inhibitors for 24 hr, and ATP content was measured using a luminescence-based assay. Error bars indicate SD; *p < 0.05 compared to untreated cancer cells.

(C) Effect of GAPDS or 6-OHDA treatment on HCT116 human colon carcinoma cell viability under normoxia and hypoxia. Cells were treated with compound for 48 hr. Error bars indicate SD; *p < 0.05 compared to 6-OHDA-treated cancer cells in the same experimental group.

(D and E) Cell death assay for HCT116 human colon carcinoma cells treated with GAPDS or 6-OHDA under normoxia (D) or hypoxia (E). Cells were treated with the compound of interest for 48 hr. Error bars indicate SD; *p < 0.05 compared to untreated cancer cells.

tumorigenic mechanisms (Guo et al., 2013). It is also known that some diabetes drugs, such as metformin, are effective against cancer (Gallagher and LeRoith, 2011). Therefore, we assessed the anticancer properties of GAPDS, using cell-based assays, biochemical analyses, and animal models. Our results indicate that GAPDS is a potent anticancer agent that inhibits both the primary and secondary functions of GAPDH. Moreover, our findings demonstrate that GAPDS is an effective chemical probe for studying GAPDH moonlighting.

RESULTS

GAPDS Inhibits GAPDH Activity and Reduces ATP Level in Cancer Cells

The chemical structures of compounds used in this study are shown in Figure S1 (available online). As our first analysis, we measured the effect of GAPDS treatment on GAPDH activity, ATP levels, and cell viability in HCT116 human colon cancer cells (Figures 1A–1E). GAPDS was compared with the known GAPDH inhibitors, iodoacetamide and 6-hydroxydopamine (6-OHDA) (Hayes and Tipton, 2002; Schmidt and Dringen, 2009). We analyzed GAPDH activity and ATP levels

at 24 hr treatment and cell viability at 48 hr treatment. These time points were chosen because the effects of GAPDH inhibitors may be influenced by the induction of cell death. For example, the nuclear localization of GAPDH and reduced GAPDH activity occurs during apoptosis (Fuchs et al., 2004; Ishitani et al., 1998). In addition, ATP levels are linked to the apoptotic process (Eguchi et al., 1997).

The previous report of GAPDS treatment in adipocytes used a concentration of 10 μM (Min et al., 2007). We observed that GAPDS inhibits GAPDH activity in HCT116 cells at a 10 μM treatment concentration and this inhibition increases up to a treatment concentration of 100 μM (Figure 1A). At these concentrations, the inhibition of GAPDH activity by GAPDS was greater than the inhibition produced by iodoacetamide treatment, but less than the inhibition produced by 6-OHDA. This difference between GAPDS and iodoacetamide treatment was also observed in ATP levels (Figure 1B). GAPDS, iodoacetamide and 6-OHDA treatment significantly reduced cellular ATP, but GAPDS and 6-OHDA produced a significantly greater reduction compared to iodoacetamide. Therefore, for our subsequent analyses in cells, we compared GAPDS with the more potent GAPDH inhibitor, 6-OHDA.

Compound GAPDS Induces Cancer Cell Death

To assess the effect of GAPDS on cancer cell viability in normoxic and hypoxic conditions, we induced hypoxia pharmacologically by exposure to cobalt chloride (Wu and Yotnda, 2011). Glycolysis inhibitors show greater effectiveness under hypoxic conditions (Pelicano et al., 2006). We observed that treatment with GAPDS produced a greater reduction in cell
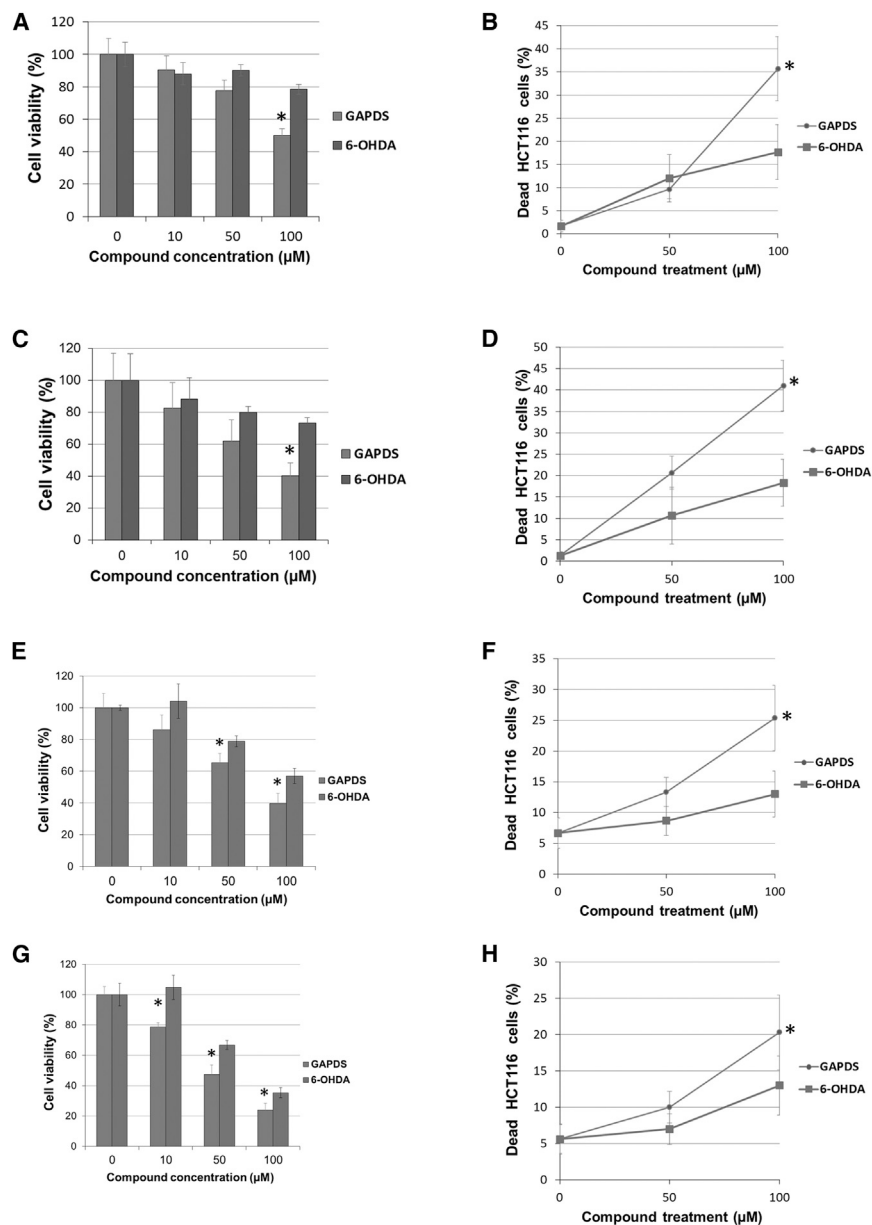
Figure 2. GAPDS Treatment Reduces Cell Viability in Different Cancer Cell Types

(A) Effect of GAPDS or 6-OHDA treatment on HT29 human colon carcinoma cell viability. Cells were treated with compound for 48 hr. Error bars indicate SD; *p < 0.05, compared to 6-OHDA-treated cancer cells in the same experimental group.

(B) Cell death assay for HT29 cells treated with GAPDS or 6-OHDA under normoxia. Cells were treated with compound for 48 hr. Error bars indicate SD; *p < 0.05, compared to 6-OHDA-treated cancer cells in the same experimental group.

(C) Effect of GAPDS or 6-OHDA treatment on HeLa human cervical carcinoma cell viability. Cells were treated with compound for 48 hr. Error bars indicate SD; *p < 0.05, compared to 6-OHDA-treated cancer cells in the same experimental group.

(D) Cell death assay for HeLa cells treated with GAPDS or 6-OHDA under normoxia. Cells were treated with compound for 48 hr. Error bars indicate SD; *p < 0.05, compared to 6-OHDA-treated cancer cells in the same experimental group.

(E) Effect of GAPDS or 6-OHDA treatment on HCT116 cell viability under hypoxia induced by treatment with 500 μM deferoxamine mesylate for 16 hr. Cells were then treated with compound for 48 hr. Error bars indicate SD; *p < 0.05, compared to 6-OHDA-treated cancer cells in the same experimental group.

(F) Cell death assay for HCT116 cells treated with GAPDS or 6-OHDA under hypoxia induced by deferoxamine mesylate. Cells were treated with compound of interest for 48 hr. Error bars indicate SD; *p < 0.05, compared to untreated cancer cells.

(G) Effect of GAPDS or 6-OHDA treatment on HCT116 human colon carcinoma cell viability under hypoxia induced by treatment with 50 μM 2,2′-dipyridyl for 18 hr. Cells were then treated with compound for 48 hr. Error bars indicate SD; *p < 0.05, compared to 6-OHDA-treated cancer cells in the same experimental group.

(H) Cell death assay for HCT116 cells treated with GAPDS or 6-OHDA under hypoxia induced by 2,2′-dipyridyl. Cells were treated with the compound of interest for 48 hr. Error bars indicate SD; *p < 0.05, compared to untreated cancer cells.

viability compared to 6-OHDA (Figure 1C). This finding was observed under both normoxia and hypoxia. However, cells were more resistant under hypoxia. Therefore, to ascertain if GAPDS treatment induced cell death under hypoxia, rather than inhibiting proliferation, we measured trypan blue exclusion. GAPDS treatment significantly increased cell death in HCT116 cells under normoxia and hypoxia compared to 6-OHDA (Figures 1D–1E). To confirm that GAPDS shows greater activity against cancer cells than 6-OHDA, we tested two other cancer cell types: a second human colon carcinoma cell line (HT29) and human cervical carcinoma (HeLa). We found that GAPDS treatment produced a greater reduction in HT29 and HeLa viability compared to 6-OHDA (Figures 2A–2D). The effect of GAPDS and 6-OHDA on cells under hypoxia was confirmed using two additional methods for hypoxic induction: treatment with deferoxamine mesylate (Yang et al., 2009) or with 2,2′-dipyridyl

(Kuphal et al., 2013). Similar to the method used with cobalt chloride, both methods are also based on modifying the levels of free iron. It was observed that GAPDS retained its greater effectiveness at reducing cell viability compared to 6-OHDA (Figures 2E–2H). To characterize how GAPDS exerts its anticancer effect, we used flow cytometric analysis of cell cycle status (Figure S2). It was observed that GAPDS treatment under normoxia increased the proportion of HCT116 cells in the G2/M phase, indicating that cell proliferation became blocked at this stage of the cell cycle. A similar effect was observed when cells were treated with 6-OHDA (Figure S2).

GAPDS Induces GAPDH Degradation and Downregulates Tubulin Expression in Cells

To further characterize the effect of GAPDS treatment in HCT116 cells, we measured the expression of GAPDH and markers of
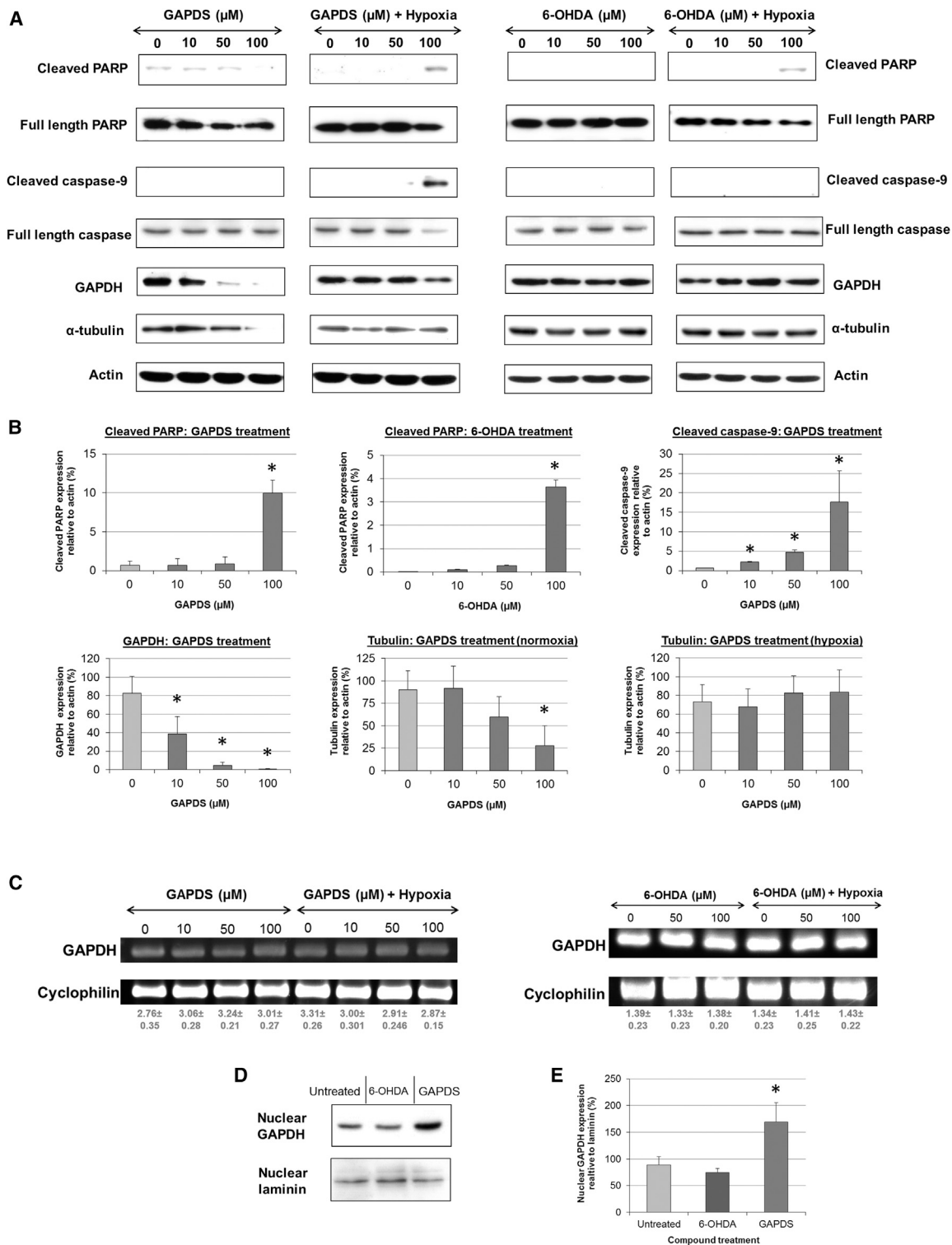
Figure 3. GAPDS Induces the Expression of Apoptosis Markers and Reduces Tubulin Expression in Cancer Cells

(A) Western blot analysis of cleaved PARP, full-length PARP, cleaved caspase-9, full-length caspase, GAPDH, α-tubulin, and actin in HCT116 human colon carcinoma cells after 48 hr compound treatment.

(B) Densitometry analysis shows average change in band intensity for three western blots (error bars indicate SD; *p < 0.05 for altered expression, compared to untreated cells). Actin was used for normalization of protein loading. Western blots for GAPDH and α-tubulin in GAPDS-treated cells were four experimental repeats.

(legend continued on next page)

apoptosis using western blot analysis (Figures 3A and 3B). The apoptosis marker, cleaved enzyme poly (ADP-ribose) polymerase (PARP) (Tewari et al., 1995), did not show any change in expression in GAPDS-treated cells under normoxia. However, the induction of hypoxia produced an increase in cleaved PARP after GAPDS treatment. We observed that treatment with 6-OHDA also produced an increase in PARP under hypoxia, but not normoxia. Expression of the apoptosis marker, cleaved caspase-9 (Li et al., 1997), also increased in GAPDS-treated cells under hypoxia, but not normoxia (Figures 3A and 3B). In contrast, there was no increase in cleaved caspase-9 expression in cells treated with 6-OHDA.

Interestingly, we observed that GAPDH expression decreased in HCT116 cells treated with GAPDS (Figures 3A and 3B). Moreover, 6-OHDA treatment did not affect GAPDH expression. The ability of GAPDS to reduce the expression of GAPDH appeared to be specific for this glycolytic enzyme, because GAPDS-treated cells showed no reduction in the expression of the downstream glycolytic enzyme, enolase (Figure S3). Furthermore, GAPDS treatment under normoxia also reduced the expression of tubulin (Figures 3A and 3B).

To assess whether the reduction in GAPDH protein levels after GAPDS treatment is caused by decreased protein expression, we carried out RT-PCR analysis of GAPDH mRNA expression (Figure 3C). It was observed that GAPDH messenger RNA (mRNA) expression stayed constant after treatment with GAPDS or 6-OHDA. GAPDH is known to undergo nuclear localization in response to various stimuli. Therefore, we assessed the effect of GAPDS treatment on nuclear levels of GAPDH (Figures 3D and 3E). It was observed that treatment with GAPDS, but not 6-OHDA, significantly increased the nuclear localization of GAPDH.

GAPDS Blocks Cell Migration and Induces Cytoskeletal Modification

In consequence of the finding that GAPDS treatment induces tubulin downregulation, we assessed the effect of this compound on cell motility. As a first test, we measured HCT116 cell invasion after treatment with GAPDS or 6-OHDA. It was observed that GAPDS treatment reduced invasion, whereas treatment with 6-OHDA had no effect (Figures 4A and 4B). This difference between the two compounds could be observed at a 10 μM treatment concentration, compared to the 50 μM treatment concentration used to inhibit cell viability (Figure 1C). To confirm that the effect of GAPDS on invasion is not restricted to one cancer cell line, we measured invasion in MBA-MD-231 human breast carcinoma cells. It was observed that treatment with GAPDS, but not 6-OHDA, also inhibited invasion in these cells (Figures 4C and 4D). To visualize migrating cells after compound treatment, we carried out the wound healing assay. It was observed that GAPDS reduced cell motility, whereas 6-OHDA treatment produced no significant effect (Figures 4E and S4). The morphology of compound-treated cells was assessed by

light microscopy, which indicated that GAPDS-treated cells did not form pseudopodia at the cell membrane (Figure S4).

Similarly to compound GAPDS, it is known that O-GlcNAcylation also disrupts the GAPDH tetramer and induces nuclear localization (Park et al., 2009). Therefore, we induced O-GlcNAcylation of cellular proteins using two methods; treatment with O-(2-acetamido-2-deoxy-D-glucopyranosylidene)amino N-phenyl carbamate (PUGNAc) or glucosamine (Champattanachai et al., 2007; Haltiwanger et al., 1998). This would test if the effect of GAPDS on GAPDH quaternary structure is responsible for the inhibition of cell motility and invasion. It was observed that treatment with glucosamine, but not PUGNAc, inhibited HCT116 cell invasion (Figures 4F and 4G). As a positive control, we used the compound LY294002, which inhibits cell invasion by blocking the phosphatidylinositol 3-kinase (PI3K) signaling pathway. To confirm the effect of glucosamine on cell motility, we carried out the wound healing assay. It was observed that treatment with glucosamine inhibited cell motility in the wound healing assay (Figure 4H).

In consequence of these results, we checked the status of the cytoskeleton in GAPDS-treated HCT116 cells using Texas Red-labeled phalloidin, which binds to actin. It was observed that GAPDS treatment prevented actin polymerization at the leading edge of the cell membrane (Figure 5A). We also assessed the effect of PUGNAc or glucosamine treatment (Figure 5B). It was observed that treatment with glucosamine, but not PUGNAc, prevented actin polymerization at the leading edge of the cell membrane.

Because of our finding that GAPDS treatment disrupts cell motility, we tested cell viability after combined treatment with another anticancer drug that targets the cytoskeleton. The drug, Taxol, was chosen for this experiment because it is a relatively well-characterized and widely used anticancer agent (Cragg, 1998). It was observed that treatment with both GAPDS and Taxol produced a synergistic effect on cell viability (Figure 5C).

GAPDH Regulates Tubulin Expression in Cancer Cells

Our data indicated that GAPDS-treated HCT116 cells showed decreased levels of GAPDH and tubulin expression (Figures 3A and 3B). Previous research has shown that GAPDH interacts with the cytoskeleton and regulates microtubule polymerization (Andrade et al., 2004). This relationship between GAPDH and tubulin expression was confirmed using small interfering RNA (siRNA)-mediated knockdown of GAPDH expression (Figures 5D–5G). Reduced GAPDH activity after siRNA treatment was detected using the KDalert GAPDH Assay Kit (Invitrogen), which has been designed to optimize GAPDH siRNA treatment (Figure 5E). In addition, knockdown of GAPDH expression after siRNA treatment was detected by western blot analysis (Figure 5G). It was observed that GAPDH gene knockdown produced a reduction in tubulin expression (Figures 5D and 5F).

(C) RT-PCR analysis of GAPDH mRNA expression after 48 hr treatment with GAPDS or 6-OHDA under normoxia or hypoxia. Cyclophilin was used for normalization of the RT-PCR reaction. The numbers in red below each band show densitometric analysis of PCR product intensity.
(D) Western blot analysis of nuclear localized GAPDH in HCT116 cells after treated with 100 μM 6-OHDA or GAPDS for 48 hr.
(E) Densitometry analysis shows average change in band intensity for three western blots (error bars indicate SD; *p < 0.05 for altered expression, compared to untreated cells). Laminin was used for normalization of protein loading.
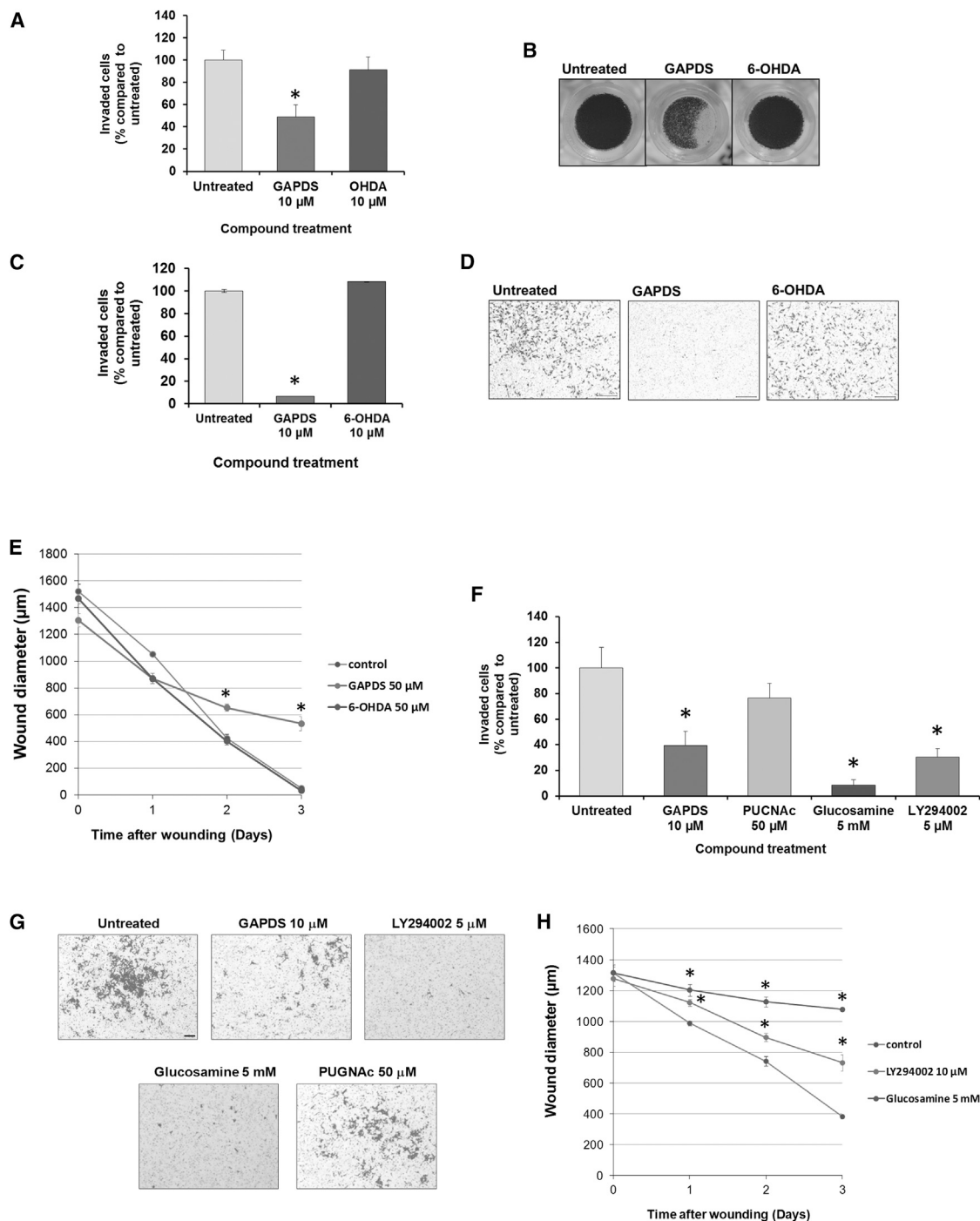
Figure 4. GAPDS Inhibits Cancer Cell Migration and Invasion

(A) HCT116 human colon carcinoma invasion after treatment with GAPDS or 6-OHDA. Error bars indicate SD; *p < 0.05, compared to untreated cells.

(B) Representative image of transwells stained with crystal violet to visualize invaded cells.

(C) MBA-MD-231 human breast adenocarcinoma cell invasion after treatment with GAPDS or 6-OHDA. Error bars indicate SD; *p < 0.05, compared to untreated cells.

(D) Representative images of invaded cancer cells stained with crystal violet. Scale bar, 100 μm.

(E) Quantification of wound healing by HCT116 cells after treatment with GAPDS or 6-OHDA. Error bars indicate SD; *p < 0.05, compared to 6-OHDA-treated cells.

(F) HCT116 cell invasion after treatment with GAPDS, PUGNAc, glucosamine, or LY294002. Error bars indicate SD; *p < 0.05, compared to untreated cells.

(G) Representative images of invaded cancer cells stained with crystal violet. Scale bar, 50 μm.

(H) Quantification of wound healing by HCT116 cells after treatment with glucosamine or LY294002. Error bars indicate SD; *p < 0.05, compared to untreated cells.

GAPDS Shows Effective Anticancer Activity In Vivo

To make an assessment of the anticancer effect of GAPDS in vivo, we selected the zebrafish (*Danio rerio*) human tumor xenograft model, which has become established as a system for testing the effect of drug candidates on cancer cell migration in host tissues (Jung et al., 2012; Konantz et al., 2012). This assay also provides a vertebrate platform for predicting toxicological effects in humans (Lee et al., 2013; Sipes et al., 2011). It was observed that GAPDS-treated embryos remained viable and showed normal developmental "landmarks" (Figure S5).

Using this model, we observed that GAPDS treatment blocked human HCT116 cell dissemination and invasion in vivo (Figure 6A). Xenografted cancer cells remained restricted at the transplantation site. In contrast, it was observed that treatment with 6-OHDA did not block the dissemination of xenografted cells, which retained their metastatic potential and could be visualized throughout the host body. This difference in the anticancer activity of GAPDS and 6-OHDA was confirmed by quantifying cell dissemination (Figure 6B).

To validate that GAPDS is effective in mammals, we tested this compound in a mouse syngeneic subcutaneous tumor model (Figure S5) (Darro et al., 2005). Tumor progression was assessed by in vivo imaging 10 days after transplantation of syngeneic CT26 colon cancer cells, and it was observed that one out of five mice developed a detectable tumor in the GAPDS-treated group, compared to four out of five mice in the 6-OHDA- or saline-treated groups. At 17 days posttransplantation, mice were sacrificed, and tumors were excised from 6-OHDA-treated mice were found to be smaller than tumors in the untreated mice. For the GAPDS-treated mice, it was observed that one tumor was of a size similar to tumors in the untreated group. However, three tumors were in the same size range as those in 6-OHDA-treated mice, and one GAPDS-treated mouse had no detectable subcutaneous tumor formation. Analysis of liver and spleen weight indicated that GAPDS or 6-OHDA treatment had no effect on liver mass. However, it was observed that 6-OHDA treatment induced a significant decrease in spleen mass (Figure S5).

DISCUSSION

Glycolytic enzymes are attractive targets for cancer drug development. In this study, our results show that the GAPDH targeting triazine, GAPDS, is a potent anticancer compound that reduces cytoplasmic levels of GAPDH, leading to reduced cancer cell motility and decreased levels of tubulin.

We observed that GAPDS reduced cancer cell viability at a treatment concentration of 50 μM and cell invasion at a concentration of 10 μM (Figures 1 and 4). This compares favorably with other known glycolysis inhibitors that target cancer cells. For example, the glycolysis inhibitor 3-BrPa, which inhibits hexokinase, is used in the 100–300 μM concentration range, and 2-deoxyglucose is used in the millimolar concentration range (Xu et al., 2005; Zhang et al., 2006).

Our western blot analysis showed that increased expression of the apoptosis marker cleaved PARP occurred in GAPDS- or 6-OHDA-treated cells, while expression of the apoptosis marker cleaved caspase-9 could only be detected in GAPDS-treated cancer cells (Figure 3). This finding suggests that there are differences in the mechanism by which these compounds induce cell death. For example, there are instances where apoptosis proceeds with PARP cleavage independently of caspase-9 cleavage, such as UV-induced apoptosis in breast adenocarcinoma cell (Ferguson et al., 2003). Characterizing this potential difference in the induction of apoptosis could be an avenue for further investigation. The ability of GAPDS to induce cancer cell death under hypoxia is also of interest, because the hypoxic environment is known to favor the survival of cancer stem cells and render other cancer drugs less effective (Xu et al., 2005). Moreover, the HCT116 cell line used in our study also possesses cancer stem cell qualities (Yeung et al., 2010). To induce hypoxia, we used chemical treatment with cobalt chloride, which has been validated in previous studies (Wu and Yotnda, 2011; Yuan et al., 2003). We chose this method because it allows the experimenter to open the culture dish without affecting the hypoxic condition, which is suitable for testing candidate compounds (Wu and Yotnda, 2011). However, to confirm our results that GAPDS is effective against cancer cells, we used two additional methods for producing hypoxia: treatment with deferoxamine mesylate or treatment with 2,2′-dipyridyl (Figures 2E–2H) (Kuphal et al., 2013; Martens et al., 2007; Spinella et al., 2010; Yang et al., 2009).

We observed that GAPDS treatment markedly reduced GAPDH levels in the cytoplasm of cancer cells (Figure 3A). The specificity of this effect was signified by the finding that GAPDS treatment did not affect the expression of the downstream glycolytic enzyme, enolase. A number of other small molecules have been shown to bind GAPDH and affect its higher order enzyme structure, such as the antidiabetic compound demethylasterriquinone B1 and the saframycin class of natural products (Kim et al., 2007; Xing et al., 2004). However, GAPDS can directly bind to GAPDH and dramatically reduce cytoplasmic levels in cancer cells, thus blocking any secondary moonlighting-associated functions of this enzyme in the cytoplasm (the saframycin class of natural products increased nuclear localization of GAPDH, but cytoplasmic levels were not significantly altered). We also observed that GAPDH expression is less affected by GAPDS treatment under hypoxia (Figure 3). It can be speculated that this is due to the increased expression of GAPDH, which is known to occur in the hypoxic environment (Xu et al., 2005).

An interesting finding from our results is the ability of GAPDS to inhibit cancer cell invasion and reduce tubulin levels (Figures 3, 4, and 5), which was not observed after treatment with the inhibitor of GAPDH enzyme activity, 6-OHDA. This finding may be due to the different mechanisms by which these small molecules bind GAPDH. 6-OHDA oxidizes sulphydryl groups in GAPDH to block enzyme activity (Hayes and Tipton, 2002). In contrast, GAPDS prevents the tetramerization of GAPDH and segregates the enzyme complex into monomers. Therefore, it can be speculated that the ability of GAPDS to inhibit GAPDH tetramerization is linked to the effects of this compound on cell motility and invasion. This inhibition of GAPDH tetramerization reduces the cytoplasmic levels of GAPDH in colon cancer cells. As shown by our analysis of GAPDH gene knockdown using siRNA (Figures 5D–5G), reduced cytoplasmic levels of GAPDH produce a decrease in α-tubulin expression. This may explain the effect of compound GAPDS on cell invasion and motility. We also tested this hypothesis by blocking GAPDH tetramerization via *O*-GlcNAcylation. However, the two methods we used to induce *O*-GlcNAcylation
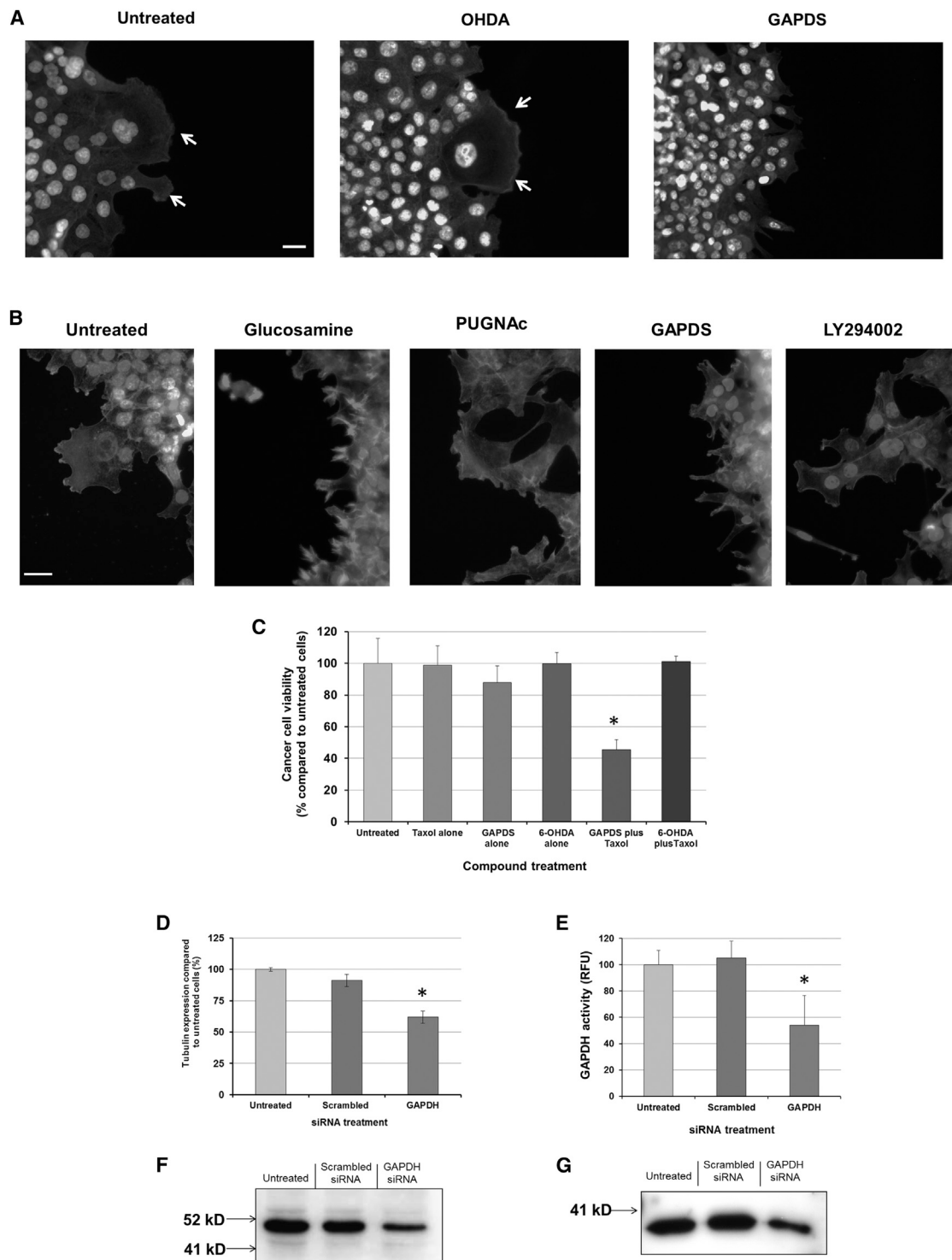
Figure 5. GAPDS Blocks Actin Polymerization and GAPDH Knockdown Decreases Tubulin Levels

(A) GAPDS-treated human HCT116 colon carcinoma cells fail to polymerize actin at the leading cell edge. Actin was visualized using fluorescent-tagged phalloidin. Areas of actin polymerization in 6-OHDA-treated or untreated cells are indicated with white arrows. DAPI was used to visualize cell nuclei. Scale bar, 10 μm.

(B) Treatment with 5 mM glucosamine, but not 50 μM PUGNAc, inhibited actin polymerization at the leading cell edge in HCT116 cells. Treatment with 5 μM LY294002 did not affect actin polymerization, in accordance with its reported property as a PI3K signaling pathway inhibitor. Scale bar, 5 μm.

(C) GAPDS, but not 6-OHDA, shows synergy with Taxol to inhibit cancer cell viability. HCT116 cells were treated with compounds for 48 hr, as follows: 5 μM GAPDS, 5 μM 6-OHDA, and 5 nM Taxol. Error bars indicate SD; *$p < 0.05$, compared to untreated cells.

(legend continued on next page)

A **Anti-cancer activity in a human cancer xenograft model**

Control

GAPDS   6-OHDA

10 µM

50 µM

100 µM

Scale bar = 200 µm

B **Quantification of human cancer cell invasion rate *in vivo***
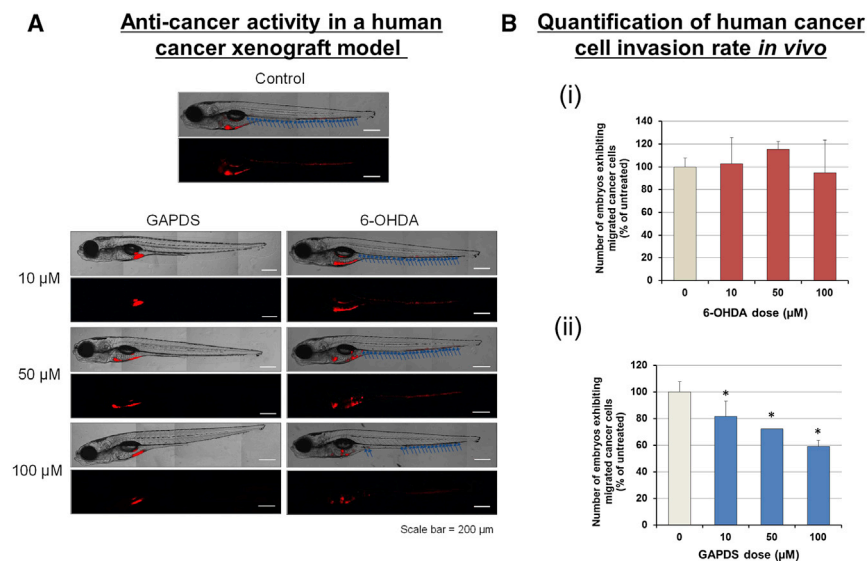
(i)

6-OHDA dose (µM)

(ii)

GAPDS dose (µM)

Figure 6. GAPDS Blocks Cancer Cell Migration In Vivo without Inducing Toxicity

(A) GAPDS treatment inhibited human HCT116 cancer cell dissemination in a human cancer xenograft model. 6-OHDA treatment did not inhibit cancer cell dissemination. Representative images of xenografted larvae are shown. The bottom panel is the fluorescence image to visualize labeled cancer cells, and the top panel is the merged fluorescence and differential interference contrast images. Disseminated cancer cells are indicated by blue arrows.

(B) Calculated invasion rate of cancer cells in xenografted larvae treated with 6-OHDA (i) or GAPDS (ii). Error bars indicate SD; *p < 0.05, compared to untreated larvae.

produced mixed results on cell invasion and cell morphology (Figures 4F–4H and 5B). Glucosamine treatment directly induces the *O*-GlcNAcylation modification on cellular proteins and effectively blocked cell invasion and motility. However, treatment with PUGNAc, which induces *O*-GlcNAcylation of cellular proteins by inhibiting *O*-GlcNAc-β-N-acetylglucosaminidase, did not affect cell invasion and cell morphology. These conflicting results may be due to the nonspecific effects of glucosamine and PUGNAc treatment in cells. For example, PUGNAc treatment has been shown to enhance cell invasion by increasing the expression of E-cadherin (Jin et al., 2013). In contrast, compound GAPDS has been shown to selectively bind to GAPDH (Min et al., 2007). We have also shown that GAPDS treatment induces GAPDH translocation to the cell nucleus (Figures 3D and 3E), which is linked to processes such as apoptosis and tumorigenesis (Colell et al., 2009; Ishitani et al., 1998). Thus, the nuclear functions of GAPDH might contribute to the effects observed after GAPDS treatment. Resolving this issue could be an interesting approach for the further study of compound GAPDS.

Drugs that target tubulin represent some of the most effective anticancer medications (Jordan, 2002). Using siRNA gene knockdown, we demonstrated that GAPDH is a regulator of tubulin expression, validating the small molecule GAPDS as a probe for characterizing the moonlighting functions of this enzyme. GAPDH is a known virulence factor linked to cell invasion into host tissues, and GAPDH colocalizes with microtubules in cancer cells (Andrade et al., 2004; Seidler, 2013). Our results show that GAPDH degradation affects cell cytoskeletal function by reducing tubulin levels, which would inhibit cell invasion. GAPDH can bind plasminogen on the cell surface and regulate

the cleavage of plasminogen into plasmin, which initiates cell invasion (Seidler, 2013). GAPDS treatment may perturb the interaction between GAPDH and plasminogen to block cancer cell invasion. However, a previous study has indicated that another glycolytic enzyme, enolase, is the major regulator of plasminogen activation (López-Alemany et al., 2003), suggesting that the interaction of GAPDH with tubulin is the mechanism linked to the anti-invasive effect of GAPDS. This concept is supported by our data showing that GAPDS has a synergistic effect with the anticancer drug, Taxol, which also affects tubulin dynamics (Figure 5C). The western blot analysis in Figure 3A indicates that, at the 10 µM treatment concentration, there is still detectable α-tubulin expression in the cancer cells. This suggests that the tubulin-binding drugs still have some effectiveness in these cells.

A previous study by Nguyen et al. (2000) reported that GAPDH localizes to pseudopodia in transformed kidney epithelial cells and that motility was inhibited by blocking glycolysis. However, our results showed that inhibition of GAPDH glycolytic function using 6-OHDA did not affect cancer cell motility (Figures 4A–4E). Instead, targeting GAPDH tetramerization using GAPDS blocked cell motility. It may be speculated that the disparity in these results is due to the different methods used to inhibit glycolysis. The study by Nguyen et al., blocked glycolysis using 2-deoxyglucose (which inhibits phosphoglucoisomerase at the second step of glycolysis) or oxamate (which is an inhibitory analog of pyruvate that reduces the activity lactate dehydrogenase). Our study used the small molecules GAPDS and 6-OHDA that specifically target GAPDH to investigate the role of this enzyme in cell motility. Thus, as a further study, it would be interesting to test whether GAPDS and/or 6-OHDA inhibits pseudopodia formation or motility in the transformed kidney epithelial cell system used by Nguyen et al.

(D) Tubulin levels in HCT116 cells treated with 120 pmol GAPDH or scrambled siRNA for 48 hr. Error bars indicate SD; *p < 0.05, compared to scrambled siRNA-treated cells. Protein lysate (30 µg) was loaded for each treatment group.

(E) GAPDH expression is downregulated by GAPDH siRNA treatment in HCT116 cells. Cells were treated with 120 pmol siRNA for 48 hr. Error bars indicate SD; *p < 0.05, compared to untreated cells.

(F) Representative western blot showing tubulin expression in siRNA-treated HCT116 cells.

(G) Representative western blot showing GAPDH expression in siRNA-treated HCT116 cells.

Our in vivo analysis showed that GAPDS is an effective anticancer agent. This was achieved without inducing developmental toxicity (Figure S5). This may be a notable result, because there are concerns that targeting GAPDH is also cytotoxic for normal cells (Krasnov et al., 2013). The zebrafish xenograft model measures human cancer cell migration and invasion into host tissues. The anti-invasive effect of GAPDS observed in vitro was recapitulated in vivo. Moreover, the observed reduction of cancer cell migration (approximately 50%) compares favorably with previous studies of well-known anticancer drugs in this model system, such as paclitaxel and 17-DMAG (Jung et al., 2012). Our mammalian analysis of GAPDS bioactivity utilized the syngeneic mouse tumor model (Figure S6). This model is valuable for testing potential antitumorigenesis agents (Darro et al., 2005). Immune-deficient mouse xenograft models lack lymphocytes, which are a component of tumor microenvironment. In syngeneic models, tumorigenesis occurs in the mouse strain in which the tumor originated and, in these immunocompetent hosts, the tumors grow relatively fast (Teicher, 2006). Our data showed that GAPDS is effective at inhibiting tumorigenesis. The GAPDH enzyme inhibitor 6-OHDA also reduced tumorgenesis in this mouse model. However, we observed that 6-OHDA-treated mice had reduced spleen weight. This may be associated with immunological dysregulation related to 6-ODHA treatment (Warrell et al., 2003). At the early stage of tumor formation, in-vivo-based imaging indicated that GAPDS is more effective than 6-OHDA. However, at the time of sacrifice, tumors dissected from GAPDS- or 6-OHDA-treated mice were of a similar size (Figure S6). We speculate that GAPDS is more effective at inhibiting the early stages of tumorigenesis in this model system. However, because this model produces relatively aggressive tumor growth, established tumors grow rapidly and "catch up" with those observed in 6-OHDA-treated mice, which can become restricted by physical constraints such as hypoxia. Thus, it would be interesting to compare GAPDS and 6-OHDA in additional mammalian models of tumorigenesis, such as the orthotopic xenograft model (Rajput et al., 2008).

The ability of GAPDS to modulate GAPDH secondary functions is significant because mitochondrial respiration remains effective in cancer cells, even though glycolysis is elevated (Koppenol et al., 2011). This suggests that inhibiting only the enzyme function of glycolytic enzymes may be inefficient for producing anticancer activity. This approach is supported by a report that the glycolytic enzyme, glucose-6-phosphate isomerase, retains its function as an autocrine cell motility factor, even when the enzyme active site is mutated (Tsutsumi et al., 2003).

Compound GAPDS was initially identified as an antidiabetic agent (Min et al., 2007). It has previously been demonstrated that some antidiabetic drugs, such as metformin, also possess anticancer activity (Gallagher and LeRoith, 2011). We previously reported that a small molecule inhibitor of enolase also possesses both antidiabetic and anticancer activity (Jung et al., 2013). We believe that our data presented herein support the further development of GAPDS as an anticancer drug. GAPDS may offer a unique opportunity for further investigation of the role of GAPDH in carcinogenesis. For example, it has recently been shown that GAPDH can bind active protein kinase B (Akt), which induces overexpression of the antiapoptosis factor, Bcl-xL and escape from caspase-independent cell death (Jacquin et al., 2013). It

would be interesting to test if GAPDS perturbs this binding to Akt and the possible consequences on cell survival.

Overall, given the recent awareness that glycolytic enzymes possess multiple moonlighting functions in cells, our results indicate that small molecule screening systems may be developed that detect the disruption of moonlighting functions in cancer drug targets. This could lead to the discovery of potent anticancer agents.

SIGNIFICANCE

The glycolytic enzyme GAPDH has been shown to carry out numerous moonlighting functions that are linked to carcinogenesis. The triazine compound GAPDH segregator (GAPDS) prevents tetramer formation by GAPDH. Compound GAPDS was previously described as a stimulator of insulin signaling in *Caenorhabditis elegans*. In this study, we show that chemical targeting of GAPDH tetramerization by GAPDS produces anticancer activity. Developing tumors create a hypoxic environment, which can reduce the effectiveness of anticancer drugs and favor the survival of cancer stem cells. Our results show that, compared to 6-OHDA, a GAPDH enzyme inhibitor that does not necessarily affect its quaternary structure, GAPDS is more effective at killing cancer cells under both normoxia and hypoxia. In addition, we discovered that GAPDS treatment blocks cell invasion and migration. This was not observed after treatment with 6-OHDA. GAPDS treatment was shown to reduce cytoplasmic levels of GAPDH and tubulin. A link between GAPDH levels and tubulin expression was confirmed using siRNA-mediated knockdown of GAPDH expression. The potent effect of GAPDS on cancer cell invasion was confirmed in an animal model of metastasis. Thus, our study shows that blocking GAPDH tetramerization reduces cytoplasmic levels of this enzyme, which also reduces tubulin expression and blocks the invasion of cancer cells in vivo. Overall, this study establishes compound GAPDS as an attractive candidate for anticancer drug development.

EXPERIMENTAL PROCEDURES

The following procedures can be found in the Supplemental Information: flow cytometry, western blotting analysis, preparation of nuclear extracts, and mouse syngeneic model of tumorigenesis.

Reagents

GAPDS was synthesized by Y.-T.C. at the National University of Singapore. Glucosamine, 6-OHDA, and iodoacetamide were purchased from Sigma-Aldrich. Deferoxamine mesylate was purchased from BioVision. We purchased 2,2′-dipyridyl and PUGNAc from Santa Cruz Biotechnology. Texas Red-X phalloidin and 1,10-dioctadecyl-3,3,3′,3′-tetramethyl-indocarbocyanine perchlorate (DiI) was purchased from Invitrogen. Antibodies for actin (sc-1615), enolase (sc-271384), GAPDH (sc-48166), α-tubulin (sc-53646), full-length caspase-9 (sc-7885), and laminin (sc-6018) were purchased from Santa Cruz Biotechnology. Antibodies for cleaved PARP (#9541L), full-length PARP (#46D11), and cleaved caspase-9 (#9501S) were purchased from Cell Signaling.

Cell Culture

HCT116 human colon carcinoma cells and HeLa human cervical carcinoma cells were cultured in 10% fetal bovine serum (FBS) and 1% P/S (5 × 10³ units per milliliter of penicillin and 5 mg/ml streptomycin) supplemented Dulbecco's

modified Eagle's medium. HT29 human colon adenocarcinoma cells, MBA-MD-231 human breast adenocarcinoma cells, and CT26 murine colon carcinoma cells were cultured in RPMI medium supplemented with 10% FBS and 1% P/S.

Hypoxia was induced in using 150 μM of 0.22 μm filtered cobalt chloride treatment, and the culture media volume was reduced by 50%, as previously described (Piret et al., 2002). The compound of interest was added 4 hr after the induction of hypoxia. The hypoxia mimetic deferoxamine mesylate was used to induce hypoxia in HCT116 cells by 500 μM treatment for 16 hr, as previously described for this cell line (Yang et al., 2009). We used 2,2′-dipyridyl to induce hypoxia by 50 μM treatment for 18 hr, as previously described (Kuphal et al., 2013).

Cell Viability and Cell Death Assays
Cell viability was measured using the tetrazolium dye methylthiotetrazole (MTT) assay (Mosmann, 1983). Cells were seeded in hexaplicate in a 96-well plate at a density of 5×10^3 cells per well. The compound of interest was added and, after 48 hr incubation, the medium was changed to MTT solution (0.5 mg/ml, final concentration) and the plate was incubated in a 37°C 5% CO_2 incubator. After 160 min incubation, 80 μl of DMSO was added. Optical density in each well was measured at 570 nm with a microplate reader (VersaMax).

Cell death was detected using the trypan blue exclusion assay, as previously described (Jung et al., 2013). Cells were prepared in a six-well plate at a density of 2×10^5 cells per well and treated with the compound of interest. After 48 hr compound treatment, cells were harvested by trypsinization and suspended in 1 ml of PBS. A 100 μl aliquot of cells was taken and stained for 5 min with an equal volume of 0.4% trypan blue. Numbers of trypan-blue-positive (dead) cells were counted using a hemocytometer.

GAPDH Activity Assay
Activity was measured using the KDalert GAPDH Assay Kit (Invitrogen), following the manufacturer's instructions. Cells were seeded in a 96-well plate at a density of 1,000 cells per well. The compound of interest was added 24 hr later. GAPDH activity was measured after 24 hr compound incubation using the fluorometric method ($\lambda_{excitation}$ = 560 nm; $\lambda_{emission}$ = 590 nm; SpectraMax GeminiEM microplate reader). We used 5 μl cell lysate for the assay.

Quantitation of Cellular ATP Level
Cellular ATP levels were measured using the StayBrite luciferase-based assay (BioVision), following the manufacturer's instructions. For the assay, cells were seeded in 96-well plates at a density of 1,000 cells per well. At 24 hr later, compounds of interest were added directly to cells. Cells were cultured with compound for 24 hr. Luminescence was measured using a multifunction microplate reader (SpectraMax GeminiEM microplate reader).

RT-PCR
Total RNA was isolated using the TRI-Solution (Bio Science Technology) and quantified with the NanoDrop 2000 spectrophotometer (Thermo Fisher Scientific) at 240/260 nm. RNA (1 μg) was reverse transcribed into complementary DNA using the AccuPower RT PreMix (Bioneer) following the manufacturer's instructions. GAPDH and cyclophilin were amplified using the AccuPower PCR PreMix (Bioneer) with the following conditions: melting at 94°C for 1 min, annealing 58.2°C for 1 min, and extension at 72°C for 30 s for 30 cycles. Primer sequences for the genes are as follows: (1) GAPDH: forward 5′-TGAT GACATCAAGAAGGTGAAG-3′ and reverse 5′-TCCTTGGAGGCCATGTA GGCCAT-3′; and (2) cyclophilin: forward 5′-GGCAAATGCTGGACCCAACA CAA-3′ and reverse 5′-CTAGGCATGGGAGGGAACAAGGA-3′.

Invasion Assay
To evaluate invasive activity, we used a modified transwell invasion assay (Youngs et al., 1997). Using 24-transwell plates (Corning), the inserts containing 8-μm-pore filters were coated with collagen type I (45 μg/30 μl per well) for the invasion assay. Briefly, carcinoma-associated fibroblasts (2×10^4 cells per well) were seeded in the bottom wells for inducing cancer cell invasion. Twenty-four hours later, cancer cells at a density of 1×10^5 cells per well were placed in the upper transwell chambers with porous filters. The cancer cells that penetrated the filter were fixed and stained with 0.25% crystal violet. Cell invasion was quantified by counting the invaded cells, which were

counted in five separate microscopic fields (100×). Mean values per filter (±SD) were calculated from three replicate filters.

Wound Healing Assay
The wound healing assay was carried out as previously described (Huang et al., 2006). Briefly, cells were seeded onto six-well plates and allowed to adhere overnight (achieving >90% confluence). The monolayer was wounded with a 200 μl plastic pipette tip. Cells were washed once, and fresh culture medium was added with or without the compound of interest. The cells were allowed to invade the wound and counted by light microscopy 12 hr later. The rate of wound healing was quantified by measuring the width of the wound at five different sites every 24 hr using light microscopy (CKX41, Olympus) and iSolution Lite 9.1 image capture software.

Assessment of Cell Morphology: Actin Visualization
Cells were seeded on glass coverslips for compound treatment. To visualize actin, cells were washed twice with PBS and fixed with 3.7% formaldehyde in PBS for 10 min. Cells were then washed two more times with PBS, and the coverslips were then placed in a glass petri dish containing 0.1% Triton X-100 in PBS for permeabilization. Cells were then washed two more times with PBS, and a blocking step was carried out by incubation with 1% BSA in PBS for 1 hr. Coverslips were then incubated with Texas Red-X phalloidin (5 μl methanolic stock solution in 200 μl PBS) for 20 min at room temperature. Coverslips were washed two more times with PBS and mounted with Fluoromount Aqueous Mounting Medium (Sigma-Aldrich). Cells were imaged by fluorescence microscopy (Leica DMI3000 B).

siRNA-Mediated Gene Silencing
siRNA-mediated knockdown of GAPDH expression was assessed using the KDalert GAPDH Assay Kit (Invitrogen), which has been designed to facilitate identification of optimal siRNA delivery conditions by assessment of GAPDH expression. In accordance with the kit manufacturer's guidelines, HCT116 cells were seeded in 96-well plates at a cell density of 10^4 cells per well. Twenty-four hours after seeding, cells were transfected with 120 pmol of siRNA, following the manufacturer's protocol provided by Santa Cruz Biotechnology (reagent volumes were scaled down from the 6-well plate format to the 96-well plate format required for the GAPDH assay). Transfected cells were used for the GAPDH assay at 48 hr posttransfection.

Zebrafish Human Cancer Cell Xenograft Model
Zebrafish were maintained by following standard procedures (Nusslein-Volhard and Dahm, 2002). Care and treatment of zebrafish were conducted in accordance with guidelines established by the Animal Care and Use Committees of the Gwangju Institute of Science and Technology, Republic of Korea. The toxicity analysis is carried out in developing zebrafish larvae, which show enhanced sensitivity to chemotoxic agents compared to adults. Zebrafish larvae can be tested in the 96-well plate format and are transparent, which means developing organ systems can be imaged by light microscopy. In accordance with previous studies of toxicological analysis (Hallare et al., 2004; Peterson et al., 2000; Sipes et al., 2011), the following developmental parameters were analyzed during embryogenesis: abnormal somite formation, tail detachment, failure to develop otoliths (ears) or eyes, defective heart development, abnormal blood circulation, delayed hatching, skeletal deformities, and the failure to swim.

For the human cancer xenograft model, zebrafish embryos were obtained using standard mating conditions and staged for cell xenoplantation at 48 hr postfertilization. Twenty embryos were used for each treatment group. After staining of cancer cells, embryos were dechorionized using microforceps and anesthetized with 0.0016% tricaine and positioned on their right side on a wet 1.0% agarose pad. Tumor cells were detached from the culture dishes using 0.05% trypsin-EDTA and washed twice with PBS at room temperature. Cells were stained with 2 μg/ml DiI diluted in PBS and washed four times: once with FBS, twice with PBS, and then once with 10% FBS diluted in PBS. Cells were kept on ice before injection. Cancer cells were counted by microscopy, suspended in 10% FBS, and injected into the center of the yolk sac using an injector (PV820 pneumatic picopump, World Precision Instruments) equipped with borosilicate glass capillaries. Injected embryos were transferred to a 96-well plate (one embryo per well) containing the drug of interest diluted in 200 μl

E3 medium (without methylene blue). The number of embryos exhibiting cancer cell dissemination from the injection site was counted by upright fluorescence microscopy (Leica DM2500 Microscope). Representative pictures were also captured using upright microscopy.

Statistical Analysis

Statistical significance was determined using the Student's t test. A p value < 0.05 was deemed to be significant. Unless otherwise stated, all data shown are representative of three experimental repeats.

SUPPLEMENTAL INFORMATION

Supplemental Information includes Supplemental Experimental Procedures and six figures and can be found with this article online at http://dx.doi.org/10.1016/j.chembiol.2014.08.017.

AUTHOR CONTRIBUTIONS

D.-W.J. and W.-H.K. designed experiments and carried out the cell-based tests of GAPDS, western analyses, RT-PCR, and the mouse tumorigenesis study; S.S. carried out the cell-based tests, siRNA analysis, and zebrafish xenograft study; E.O. carried out the zebrafish toxicology test; S.-H.Y. designed experiments; H.-H.H. and Y.-T.C. synthesized GAPDS and provided research advice; D.R.W. designed experiments and wrote the manuscript.

REFERENCES

Andrade, J., Pearce, S.T., Zhao, H., and Barroso, M. (2004). Interactions among p22, glyceraldehyde-3-phosphate dehydrogenase and microtubules. Biochem. J. *384*, 327–336.

Bagley, R.G. (Ed.). (2010). The Tumor Microenvironment (Cancer Drug Discovery and Development). (New York: Springer).

Champattanachai, V., Marchase, R.B., and Chatham, J.C. (2007). Glucosamine protects neonatal cardiomyocytes from ischemia-reperfusion injury via increased protein-associated O-GlcNAc. Am. J. Physiol. Cell Physiol. *292*, C178–C187.

Colell, A., Green, D.R., and Ricci, J.E. (2009). Novel roles for GAPDH in cell death and carcinogenesis. Cell Death Differ. *16*, 1573–1581.

Cragg, G.M. (1998). Paclitaxel (Taxol): a success story with valuable lessons for natural product drug discovery and development. Med. Res. Rev. *18*, 315–331.

Dai, R.P., Yu, F.X., Goh, S.R., Chng, H.W., Tan, Y.L., Fu, J.L., Zheng, L., and Luo, Y. (2008). Histone 2B (H2B) expression is confined to a proper NAD+/NADH redox status. J. Biol. Chem. *283*, 26894–26901.

Darro, F., Decaestecker, C., Gaussin, J.F., Mortier, S., Van Ginckel, R., and Kiss, R. (2005). Are syngeneic mouse tumor models still valuable experimental models in the field of anti-cancer drug discovery? Int. J. Oncol. *27*, 607–616.

Eguchi, Y., Shimizu, S., and Tsujimoto, Y. (1997). Intracellular ATP levels determine cell death fate by apoptosis or necrosis. Cancer Res. *57*, 1835–1840.

Ferguson, H.A., Marietta, P.M., and Van Den Berg, C.L. (2003). UV-induced apoptosis is mediated independent of caspase-9 in MCF-7 cells: a model for cytochrome c resistance. J. Biol. Chem. *278*, 45793–45800.

Fuchs, J., Podda, M., and Packer, L. (2004). Redox-Genome Interactions in Health and Disease. (New York: Marcel Dekker).

Gallagher, E.J., and LeRoith, D. (2011). Diabetes, cancer, and metformin: connections of metabolism and cell proliferation. Ann. N Y Acad. Sci. *1243*, 54–68.

Guo, C., Liu, S., and Sun, M.Z. (2013). Novel insight into the role of GAPDH playing in tumor. Clin. Transl. Oncol. *15*, 167–172.

Hallare, A.V., Köhler, H.R., and Triebskorn, R. (2004). Developmental toxicity and stress protein responses in zebrafish embryos after exposure to diclofenac and its solvent, DMSO. Chemosphere *56*, 659–666.

Haltiwanger, R.S., Grove, K., and Philipsberg, G.A. (1998). Modulation of O-linked N-acetylglucosamine levels on nuclear and cytoplasmic proteins in vivo using the peptide O-GlcNAc-beta-N-acetylglucosaminidase inhibitor O-(2-acetamido-2-deoxy-D-glucopyranosylidene)amino-N-phenylcarbamate. J. Biol. Chem. *273*, 3611–3617.

Hayes, J.P., and Tipton, K.F. (2002). Interactions of the neurotoxin 6-hydroxydopamine with glyceraldehyde-3-phosphate dehydrogenase. Toxicol. Lett. *128*, 197–206.

Huang, M.C., Chen, H.Y., Huang, H.C., Huang, J., Liang, J.T., Shen, T.L., Lin, N.Y., Ho, C.C., Cho, I.M., and Hsu, S.M. (2006). C2GnT-M is downregulated in colorectal cancer and its re-expression causes growth inhibition of colon cancer cells. Oncogene *25*, 3267–3276.

Ishitani, R., Tanaka, M., Sunaga, K., Katsube, N., and Chuang, D.M. (1998). Nuclear localization of overexpressed glyceraldehyde-3-phosphate dehydrogenase in cultured cerebellar neurons undergoing apoptosis. Mol. Pharmacol. *53*, 701–707.

Jacquin, M.A., Chiche, J., Zunino, B., Bénéteau, M., Meynet, O., Pradelli, L.A., Marchetti, S., Cornille, A., Carles, M., and Ricci, J.E. (2013). GAPDH binds to active Akt, leading to Bcl-xL increase and escape from caspase-independent cell death. Cell Death Differ. *20*, 1043–1054.

Jeffery, C.J. (2009). Moonlighting proteins—an update. Mol. Biosyst. *5*, 345–350.

Jin, F.Z., Yu, C., Zhao, D.Z., Wu, M.J., and Yang, Z. (2013). A correlation between altered O-GlcNAcylation, migration and with changes in E-cadherin levels in ovarian cancer cells. Exp. Cell Res. *319*, 1482–1490.

Jordan, M.A. (2002). Mechanism of action of antitumor drugs that interact with microtubules and tubulin. Curr. Med. Chem. Anticancer Agents *2*, 1–17.

Jung, D.W., Oh, E.S., Park, S.H., Chang, Y.T., Kim, C.H., Choi, S.Y., and Williams, D.R. (2012). A novel zebrafish human tumor xenograft model validated for anti-cancer drug screening. Mol. Biosyst. *8*, 1930–1939.

Jung, D.W., Kim, W.H., Park, S.H., Lee, J., Kim, J., Su, D., Ha, H.H., Chang, Y.T., and Williams, D.R. (2013). A unique small molecule inhibitor of enolase clarifies its role in fundamental biological processes. ACS Chem. Biol. *8*, 1271–1282.

Kim, J.W., and Dang, C.V. (2005). Multifaceted roles of glycolytic enzymes. Trends Biochem. Sci. *30*, 142–150.

Kim, H., Deng, L., Xiong, X., Hunter, W.D., Long, M.C., and Pirrung, M.C. (2007). Glyceraldehyde 3-phosphate dehydrogenase is a cellular target of the insulin mimic demethylasterriquinone B1. J. Med. Chem. *50*, 3423–3426.

Konantz, M., Balci, T.B., Hartwig, U.F., Dellaire, G., André, M.C., Berman, J.N., and Lengerke, C. (2012). Zebrafish xenografts as a tool for in vivo studies on human cancer. Ann. N Y Acad. Sci. *1266*, 124–137.

Koppenol, W.H., Bounds, P.L., and Dang, C.V. (2011). Otto Warburg's contributions to current concepts of cancer metabolism. Nat. Rev. Cancer *11*, 325–337.

Krasnov, G.S., Dmitriev, A.A., Snezhkina, A.V., and Kudryavtseva, A.V. (2013). Deregulation of glycolysis in cancer: glyceraldehyde-3-phosphate dehydrogenase as a therapeutic target. Expert Opin. Ther. Targets *17*, 681–693.

Kuphal, S., Wallner, S., and Bosserhoff, A.K. (2013). Impact of LIF (leukemia inhibitory factor) expression in malignant melanoma. Exp. Mol. Pathol. *95*, 156–165.

Lee, J., Jung, D.W., Kim, W.H., Um, J.I., Yim, S.H., Oh, W.K., and Williams, D.R. (2013). Development of a highly visual, simple, and rapid test for the discovery of novel insulin mimetics in living vertebrates. ACS Chem. Biol. 8, 1803–1814.

Li, P., Nijhawan, D., Budihardjo, I., Srinivasula, S.M., Ahmad, M., Alnemri, E.S., and Wang, X. (1997). Cytochrome c and dATP-dependent formation of Apaf-1/caspase-9 complex initiates an apoptotic protease cascade. Cell 91, 479–489.

López-Alemany, R., Longstaff, C., Hawley, S., Mirshahi, M., Fábregas, P., Jardí, M., Merton, E., Miles, L.A., and Félez, J. (2003). Inhibition of cell surface mediated plasminogen activation by a monoclonal antibody against alpha-Enolase. Am. J. Hematol. 72, 234–242.

Martens, L.K., Kirschner, K.M., Warnecke, C., and Scholz, H. (2007). Hypoxia-inducible factor-1 (HIF-1) is a transcriptional activator of the TrkB neurotrophin receptor gene. J. Biol. Chem. 282, 14379–14388.

Min, J., Kyung Kim, Y., Cipriani, P.G., Kang, M., Khersonsky, S.M., Walsh, D.P., Lee, J.Y., Niessen, S., Yates, J.R., 3rd, Gunsalus, K., et al. (2007). Forward chemical genetic approach identifies new role for GAPDH in insulin signaling. Nat. Chem. Biol. 3, 55–59.

Mosmann, T. (1983). Rapid colorimetric assay for cellular growth and survival: application to proliferation and cytotoxicity assays. J. Immunol. Methods 65, 55–63.

Nguyen, T.N., Wang, H.J., Zalzal, S., Nanci, A., and Nabi, I.R. (2000). Purification and characterization of beta-actin-rich tumor cell pseudopodia: role of glycolysis. Exp. Cell Res. 258, 171–183.

Nusslein-Volhard, C., and Dahm, R., eds. (2002). Zebrafish (The Practical Approach Series) (New York: Oxford University Press).

Park, J., Han, D., Kim, K., Kang, Y., and Kim, Y. (2009). O-GlcNAcylation disrupts glyceraldehyde-3-phosphate dehydrogenase homo-tetramer formation and mediates its nuclear translocation. Biochim. Biophys. Acta 1794, 254–262.

Pelicano, H., Martin, D.S., Xu, R.H., and Huang, P. (2006). Glycolysis inhibition for anticancer treatment. Oncogene 25, 4633–4646.

Peterson, R.T., Link, B.A., Dowling, J.E., and Schreiber, S.L. (2000). Small molecule developmental screens reveal the logic and timing of vertebrate development. Proc. Natl. Acad. Sci. USA 97, 12965–12969.

Piret, J.P., Mottet, D., Raes, M., and Michiels, C. (2002). CoCl2, a chemical inducer of hypoxia-inducible factor-1, and hypoxia reduce apoptotic cell death in hepatoma cell line HepG2. Ann. N Y Acad. Sci. 973, 443–447.

Rajput, A., Dominguez San Martin, I., Rose, R., Beko, A., Levea, C., Sharratt, E., Mazurchuk, R., Hoffman, R.M., Brattain, M.G., and Wang, J. (2008). Characterization of HCT116 human colon cancer cells in an orthotopic model. J. Surg. Res. 147, 276–281.

Schmidt, M.M., and Dringen, R. (2009). Differential effects of iodoacetamide and iodoacetate on glycolysis and glutathione metabolism of cultured astrocytes. Front. Neuroenergetics 1, 1.

Seidler, N.W. (2013). GAPDH, as a virulence factor. Adv. Exp. Med. Biol. 985, 149–178.

Sipes, N.S., Padilla, S., and Knudsen, T.B. (2011). Zebrafish: as an integrative model for twenty-first century toxicity testing. Birth Defects Res. C Embryo Today 93, 256–267.

Spinella, F., Rosanò, L., Del Duca, M., Di Castro, V., Nicotra, M.R., Natali, P.G., and Bagnato, A. (2010). Endothelin-1 inhibits prolyl hydroxylase domain 2 to activate hypoxia-inducible factor-1alpha in melanoma cells. PLoS ONE 5, e11241.

Subramanian, A., and Miller, D.M. (2000). Structural analysis of alpha-enolase. Mapping the functional domains involved in down-regulation of the c-myc protooncogene. J. Biol. Chem. 275, 5958–5965.

Teicher, B.A. (2006). Tumor models for efficacy determination. Mol. Cancer Ther. 5, 2435–2443.

Tewari, M., Quan, L.T., O'Rourke, K., Desnoyers, S., Zeng, Z., Beidler, D.R., Poirier, G.G., Salvesen, G.S., and Dixit, V.M. (1995). Yama/CPP32 beta, a mammalian homolog of CED-3, is a CrmA-inhibitable protease that cleaves the death substrate poly(ADP-ribose) polymerase. Cell 81, 801–809.

Tristan, C., Shahani, N., Sedlak, T.W., and Sawa, A. (2011). The diverse functions of GAPDH: views from different subcellular compartments. Cell. Signal. 23, 317–323.

Tsutsumi, S., Gupta, S.K., Hogan, V., Tanaka, N., Nakamura, K.T., Nabi, I.R., and Raz, A. (2003). The enzymatic activity of phosphoglucose isomerase is not required for its cytokine function. FEBS Lett. 534, 49–53.

Warburg, O., Wind, F., and Negelein, E. (1927). The metabolism of tumors in the body. J. Gen. Physiol. 8, 519–530.

Warrell, D.A., Cox, T.M., Firth, J.D., and Benz, E.J., Jr. (2003). Oxford Textbook of Medicine, Fourth Edition. (New York: Oxford University Press).

Wu, D., and Yotnda, P. (2011). Induction and testing of hypoxia in cell culture. J. Vis. Exp. (54), 2899.

Xing, C., LaPorte, J.R., Barbay, J.K., and Myers, A.G. (2004). Identification of GAPDH as a protein target of the saframycin antiproliferative agents. Proc. Natl. Acad. Sci. USA 101, 5862–5866.

Xu, R.H., Pelicano, H., Zhou, Y., Carew, J.S., Feng, L., Bhalla, K.N., Keating, M.J., and Huang, P. (2005). Inhibition of glycolysis in cancer cells: a novel strategy to overcome drug resistance associated with mitochondrial respiratory defect and hypoxia. Cancer Res. 65, 613–621.

Yang, J., Ahmed, A., Poon, E., Perusinghe, N., de Haven Brandon, A., Box, G., Valenti, M., Eccles, S., Rouschop, K., Wouters, B., and Ashcroft, M. (2009). Small-molecule activation of p53 blocks hypoxia-inducible factor 1alpha and vascular endothelial growth factor expression in vivo and leads to tumor cell apoptosis in normoxia and hypoxia. Mol. Cell. Biol. 29, 2243–2253.

Yeung, T.M., Gandhi, S.C., Wilding, J.L., Muschel, R., and Bodmer, W.F. (2010). Cancer stem cells from colorectal cancer-derived cell lines. Proc. Natl. Acad. Sci. USA 107, 3722–3727.

Youngs, S.J., Ali, S.A., Taub, D.D., and Rees, R.C. (1997). Chemokines induce migrational responses in human breast carcinoma cell lines. Int. J. Cancer 71, 257–266.

Yuan, Y., Hilliard, G., Ferguson, T., and Millhorn, D.E. (2003). Cobalt inhibits the interaction between hypoxia-inducible factor-alpha and von Hippel-Lindau protein by direct binding to hypoxia-inducible factor-alpha. J. Biol. Chem. 278, 15911–15916.

Zhang, X.D., Deslandes, E., Villedieu, M., Poulain, L., Duval, M., Gauduchon, P., Schwartz, L., and Icard, P. (2006). Effect of 2-deoxy-D-glucose on various malignant cell lines in vitro. Anticancer Res. 26 (5A), 3561–3566.